

# Frequency Range, $\log E$ , $\log P$ and Magnitude

Aleksander J. Mendecki  
Institute of Mine Seismology, Australia

## Abstract

The potency and energy range of seismic events that a system can recover is limited by its frequency range ( $f_1, f_2$ ), which is mainly determined by the capabilities of seismic sensors. In hard rock with  $v_S = 3.6$  km/s and  $\mu = 30$  GPa the largest event for which we can recover 85% of seismic potency is  $P \simeq 7.41\Delta\sigma/(10f_1)^3$ , which for  $\Delta\sigma = 3$  MPa and  $f_1 = 3$  Hz gives  $\log P=2.9$ . The smallest event for which we can recover 85% of radiated energy is  $P \simeq 100\Delta\sigma/f_2^3$ , which for  $f_2 = 1$  kHz gives  $\log P=-0.5$ . While 15% underestimates of seismic potency do not have a significant effect on potency or energy based magnitudes, it has a notable effect on the apparent stress and the apparent volume. The problem may be alleviated by partially correcting for the limited bandwidth, but the best strategy is to select the correct sensors.

The most appropriate measure of the strength of a seismic source is the radiated seismic energy since it controls the high frequency radiation and drives strong ground motion. Therefore  $E$ , or  $\log E$ , should be the base of a magnitude scale, as originally intended by *Gutenberg and Richter (1956a)*,  $m_S = 2/3\log E - 3.2$ , where  $m_S$  is the surface wave magnitude of larger earthquakes. The *Gutenberg and Richter* relation was later corrected by *Choy and Boatwright (1995)* who calculated the radiated energy from the velocity spectra of 397 earthquakes with  $m \geq 5.8$  and, assuming the constant slope of  $2/3$ , obtained  $m_e = 2/3\log E - 2.9$ . That indicates that the Gutenberg-Richter formula may overestimate the radiated energy by a factor of 2.5 on average. The energy measure of the strength of an earthquake,  $K=\log E$ , was adopted in Russia (*Rautian, 1960*) and then in Polish coal mines (*Gibowicz, 1963, Wierzchowska and Dubinski, 1973*).

The routine estimation of seismic energy from waveforms is demanding. It requires triaxial recordings and the integration of the energy flux of the velocity squared spectra of body waves over the duration of the source process and corrections for the effects of geometric spreading, attenuation, radiation pattern and site. It requires far-field recordings over a wide frequency range, preferably from  $0.2f_0$  to  $10f_0$ , where  $f_0$  is the corner frequency of the displacement spectrum, see Figure 2 and 3.

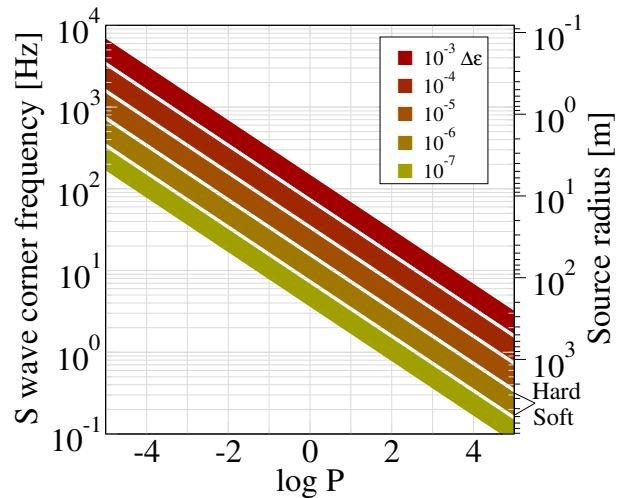


Figure 1: Expected S-wave corner frequency and source radius as a function of  $\log P$  for different strain drops and rock type (after *Mountfort and Mendecki, 1997*).

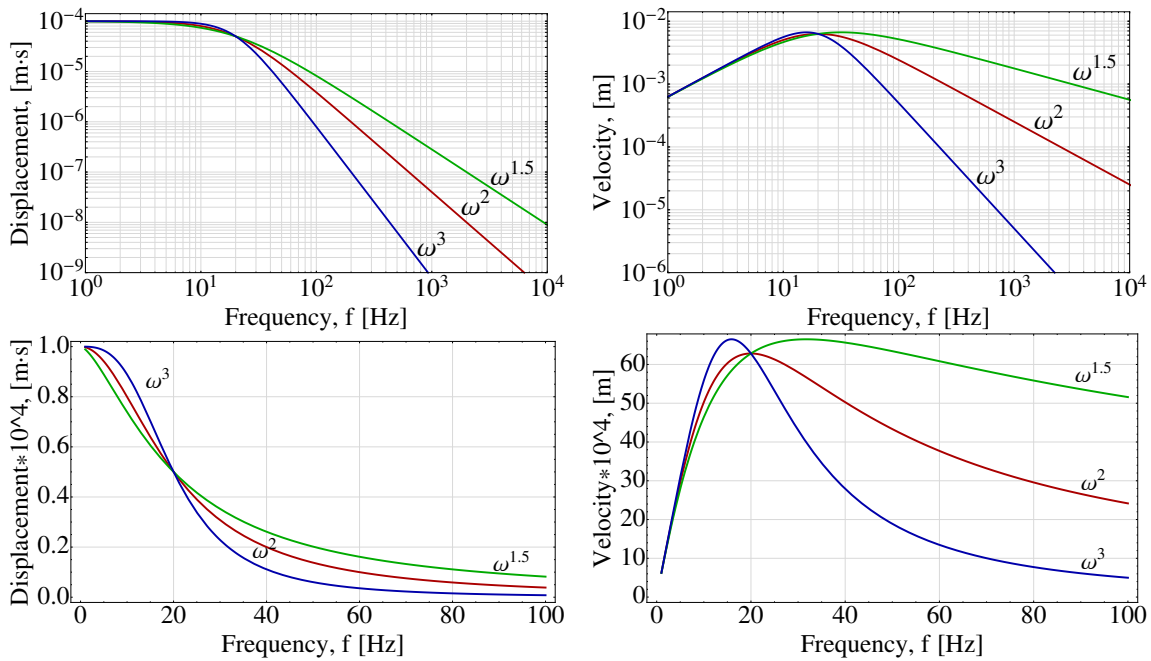


Figure 2: log-log graphs of the theoretical displacement spectrum (*top left*) and velocity spectrum (*top right*) for the  $\omega^2$ -model (black solid line),  $\omega^{1.5}$  (grey dashed) and  $\omega^3$  (black dashed) for a  $\log P=1.2$  event and  $f_0 = 20$  Hz. The *bottom left* and *right* show the first 100 Hz of these spectra in a linear scale to demonstrate their asymmetry.

The rate of seismic activity in mines does not always allow for careful, time consuming processing with proper corrections for attenuation and site effects, which are notoriously difficult at higher frequencies, specifically in mines where rock mass properties are being altered. Most of the seismic energy is radiated at frequencies above  $f_0$  and for small events the higher frequencies may be filtered out by sensors. Also, due to the limited aperture of mine seismic networks, spectra of larger events recorded by sensors close to sources are contaminated by the near or intermediate fields of seismic radiation.

Seismic potency of a single dislocation source is the product of an average slip and source area,  $P = \bar{u}A$  (Ben-Menahem and Singh, 1981). For a complex source, potency is the product of the source strain and the source volume,  $P = \Delta\epsilon V$  (Madariaga, 1979), where  $\Delta\epsilon = \Delta\sigma/\mu$ ,  $\Delta\sigma$  is an averaged stress drop and  $\mu$  is the rigidity of the rock mass surrounding the source. Seismic moment  $M = \mu P = \mu\Delta\epsilon V = \Delta\sigma V$ .

Assuming the relation between the S-wave corner frequency,  $f_0$ , S-wave velocity,  $v_S$ , and source radius,  $r = 0.3v_S/f_0$ , (Brune *et al.*, 1979), and that  $P = 16\Delta\epsilon r^3/7$  (Eshelby, 1957; Keilis-Borok, 1959), we can derive the following simple relation

$$f_0 = 0.395 (\Delta\epsilon/P)^{1/3}. \quad (1)$$

Since  $v_S = (\mu/\rho)^{1/2}$  one can construct a nomogram, see Figure 1, representing the relations between these variables for hard rocks, defined here by  $\mu = 37$  GPa,  $\rho = 2700$  kg/m<sup>3</sup> and  $v_S = 3700$  m/s (top of the band) and for soft rocks by  $\mu = 7.2$  GPa,  $\rho = 1800$  kg/m<sup>3</sup> and  $v_S = 2000$  m/s (bottom of the band).

Seismic potency is a parameter that is observable at the low frequency asymptote of the displacement spectrum where corrections for attenuation and scattering are less difficult and, as a result, its estimate is less uncertain than that of seismic energy. An average uncertainties in routine estimates of seismic potency are less than 50%, while they can be over 80% for seismic energy. A simple solution for magnitude then, at least in hard rock mines, is to utilise one of the moment or potency based magnitude relations, see Table 1.

Table 1: Moment magnitudes relations recalculated to potency for  $\mu = 30$  GPa.

Author	Domain of validity	Equation
Wyss and Brune (1968)	$3 < m < 6$	$m = 0.59 \log P + 1.4$
Aki (1969)	$3 < m < 5$	$m = 2/3 \log P + 1.12$
Gibowicz (1975)	$m < 4.5$	$m = \log P + 0.32$
Bakun and Lindh (1977)	$m < 3.5$	$m = 0.83 \log P + 0.4$
Hanks and Kanamori (1979)	$3 < m < 7.5$	$m_{HK} = 2/3 \log P + 0.92$
Ben-Zion and Zhu (2002)	$m < 3.5$	$m = \log P + 0.72$

The most frequently used moment-magnitude is the *Hanks and Kanamori* (1979) relation, which for seismic potency gives  $m_{HK} = 2/3 \log P + 0.92$ . The  $m_{HK}$  is consistent with the *Gutenberg and Richter* empirical relation between seismic energy  $E$  and the  $m_S$  for intermediate and larger earthquakes. It assumes a constant apparent stress  $\sigma_A = E/P = 1.5$  MPa, which implies a slope of 1.0 on the  $\log E$  vs  $\log P$  plot. For  $\sigma_A = 1.5$  MPa the *Boatwright and Choy* formula translates to potency magnitude as  $m_e = 2/3 \log P + 1.2$ . Note that for small earthquakes  $m \sim \log P$  as opposed to  $m \sim 2/3 \log P$ , see also *Kanamori and Anderson, 1975*.

The potency and energy range of seismic events that a system can recover is limited by its frequency range  $(f_1, f_2)$ , which is mainly determined by the capabilities of seismic sensors. Figure 3 (left) shows the recovery of seismic potency as a function of the ratio of available frequencies at the lower end of the spectrum  $f_1$ , to corner frequency  $f_0$  for  $\omega^n$ -models,  $n = 1.5, 2$  and  $3$ , where the displacement spectrum is

$$u(n, f) = \frac{\Omega_0}{1 + (f/f_0)^n}, \quad (2)$$

where  $\Omega_0$  is the zero frequency limit of the displacement spectrum. The displacement power spectrum is  $P_u(n) = 2 \int_0^\infty [u(n, f)]^2 df = 2\pi\Omega_0^2 f_0 (n-1) / [n^2 \sin(\pi/n)]$ . The potency recovery then can be defined as  $P(f=f_1)/P(f=0)$ .

For the conventional  $\omega^2$ -model, i.e.  $n = 2$ , it shows that at  $0.2f_0$  we can recover 96%, at  $0.42f_0$  85% and at the corner frequency only 50% of seismic potency respectively. Assuming a circular source with stress drop  $\Delta\sigma = (7\mu P)/(16r^3)$  (*Keilis-Borok, 1959*), corner frequency  $f_0 = 0.3v_S/r$  (*Brune et al., 1979*) and hard rock with  $v_S = 3600$  m/s and  $\mu = 30$  GPa, the potency  $P = 0.1\Delta\sigma/f_0^3$ . Therefore, the largest event for which we can recover 85% of seismic potency is  $P \simeq 7.41\Delta\sigma/(10f_1)^3$ , which for  $\Delta\sigma = 3$  MPa and  $f_1 = 4.5$  Hz is  $\log P = 2.39$  and for  $f_1 = 3$  Hz is  $\log P = 2.92$ . The 85% recovery underestimates  $\log P$  by  $\log(0.85P) = \log P - 0.07$ , and the  $m_{HK}$  by 0.047. At 50% recovery, i.e.  $f_1/f_0 = 1.0$  the  $\log P$  is underestimated by 0.3 units and the  $m_{HK}$  by 0.2.

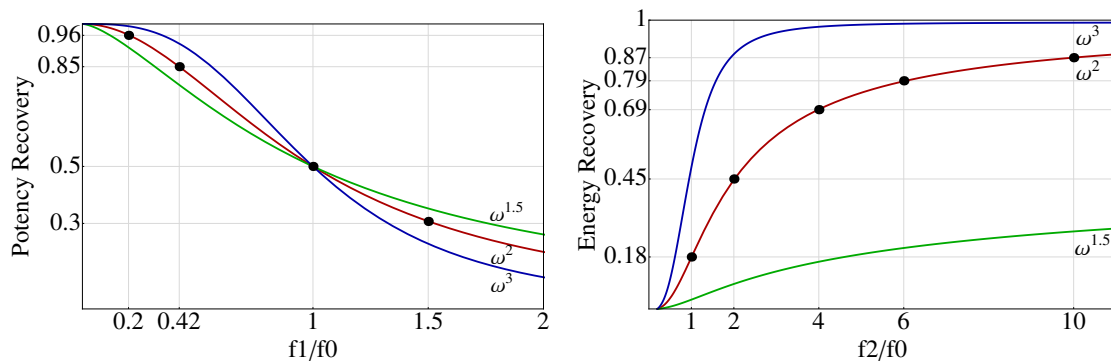


Figure 3: Recovery of seismic potency as a function of  $f_1/f_0$  (left) and radiated energy  $E(0.2f_0, f_2)/E(f_1 = 0, \infty)$  as a function of  $f_2/f_0$  (right) for the  $\omega^2$ -model (thick solid line), the  $\omega^{1.5}$  (grey dashed) and the  $\omega^3$  (black dashed). To secure a finite energy the recovery for the  $\omega^{1.5}$ -model is defined as  $E(0.2f_0, f_2)/E(f_1 = 0.01f_0, f_2 = 100f_0)$ . The large black dots on the  $\omega^2$ -model indicate particular recoveries of potency and energy.

Seismic radiated energy is proportional to the velocity power spectrum

$$E \sim P_v(n) = 2 \int_0^{\infty} [\dot{u}(n, f)]^2 df = 2 \int_0^{\infty} \left[ \frac{2\pi f \Omega_0}{1 + (f/f_0)^n} \right]^2 df = \frac{(2\pi f_0)^3 \Omega_0^2 (n-3)}{n^2 \sin(3\pi/n)} \quad (3)$$

Note that for  $n \leq 1.5$  the integral defining  $P_v(n=1.5)$  diverges. The predominant frequency at which the maximum energy is radiated  $f_E$ , is at the maximum of the velocity power spectrum. Taking  $\partial \dot{u}(n, f)/\partial f = 0$  and solving for  $f$  gives

$$f_E(n) = \frac{1}{(n-1)^{1/n}} \cdot f_0 \quad (4)$$

Therefore for the  $\omega^2$ -model the predominant frequency is at the corner frequency,  $f_E(2) = f_0$ . For the  $\omega^3$ -model the  $f_E(3) = f_0/\sqrt[3]{2} = 0.7937f_0$  and the  $f_E(1.5) = 1.587f_0$ , see Figure 4 (left). The  $\lim_{n \rightarrow 1} f_E(n) = \infty$  and the  $\lim_{n \rightarrow \infty} f_E(n) = 1$ .

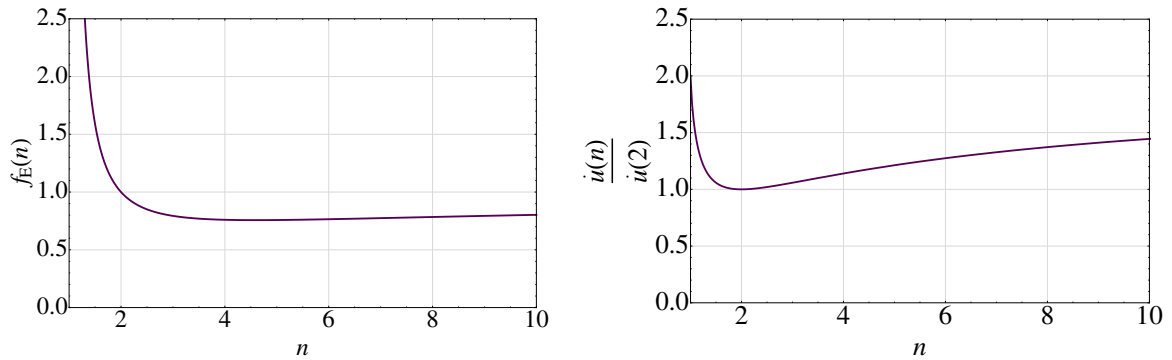


Figure 4: Predominant frequency as a function of the corner frequency for  $\omega^n$ -models (left) and the ratio of the maximum amplitude of the  $\omega^n$ -model to the  $\omega^2$  one (right).

Inserting  $f_E(n)$  into  $\dot{u}(n, f)$  gives the maximum amplitude of the velocity spectrum and the ratio of the maximum amplitude of the  $\omega^n$ -model to the  $\omega^2$  one

$$\dot{u}(n) = \frac{2\pi f_0 \Omega_0}{n} (n-1)^{\frac{n-1}{n}} \quad \dot{u}(n)/\dot{u}(2) = \frac{2}{n} (n-1)^{\frac{n-1}{n}}, \quad (5)$$

see Figure 4 (right) and Figure 2 (bottom right). The  $\lim_{n \rightarrow \infty} [\dot{u}(n)/\dot{u}(2)] = 2$  and  $\lim_{n \rightarrow 1} [\dot{u}(n)/\dot{u}(2)] = 2$ .

The energy recovery defined as  $E(f_1, f_2)/E(f_1=0, f_2=\infty)$  for the  $\omega^2$ -model gives

$$E(f_1, f_2)/E(f_1=0, f_2=\infty) = 2(B+A)/\pi, \quad (6)$$

where  $B = (f_1/f_0)/[1 + (f_1/f_0)^2] - (f_2/f_0)/[1 + (f_2/f_0)^2]$  and  $A = \arctan(f_2/f_0) - \arctan(f_1/f_0)$  (see also *Di Bona and Rovelli, 1988*).

Figure (3) (right) shows that the  $\omega^2$ -model produces 18% of energy below the corner frequency (left of  $f_2/f_0=1$ ), the  $\omega^{1.5}$ -model less than 10% while the  $\omega^3$  almost 50%. The energy recovery at Figure 3 (right) is calculated for  $f_1 = 0.2f_0$  and  $f_2$  varying from  $0.2f_0$  (0% recovery) to  $10f_0$  (87% recovery). Therefore for  $\omega^2$ -model the smallest event for which we can recover at least 85% of energy is  $P \simeq 0.1\Delta\sigma/(f_2/10)^3$ , which for  $\Delta\sigma = 3$  MPa and  $f_2 = 1000$  Hz is  $\log P = -0.5$ .

Figure 5 shows the maximum  $\log P$  for which we can measure 85% of potency as a function of  $f_1$ , and the minimum  $\log P$  for which we can measure at least 85% of radiated energy as a function of  $f_2$ .

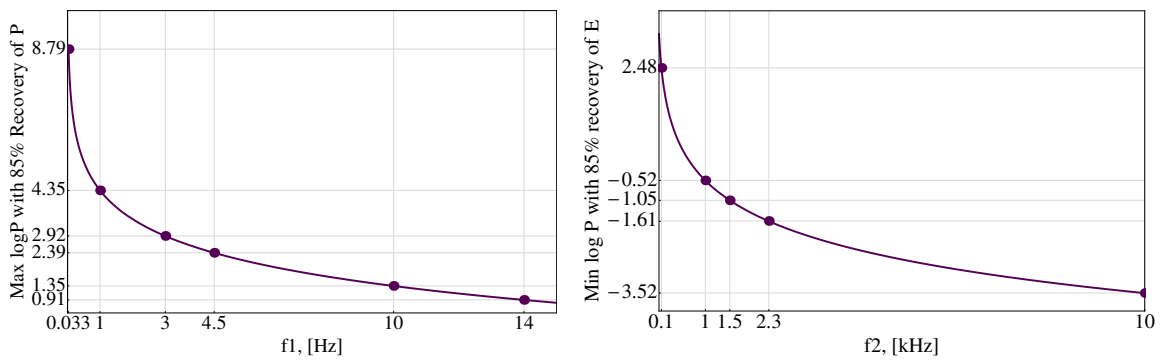


Figure 5: The maximum  $\log P$  for which we can measure at least 85% of seismic potency as a function of  $f_1$  (left), and the minimum  $\log P$  for which we can measure at least 85% of seismic energy as a function of  $f_2$  (right), both for the  $\omega^2$ -model. Typical sensor characteristics are marked by dots.

While the underestimation of seismic potency does not have a significant effect on the potency based magnitude, it has a notable effect on the estimation of the apparent stress and the apparent volume,  $V_A = \mu P^2 / E$  (Mendecki, 1993). Figure 6 illustrates the influence of the limited frequency range of four hypothetical sensors on the estimation of  $\sigma_A$  and  $V_A$ . The problem may be alleviated by correcting for the limited bandwidth while calculating the displacement and velocity power spectra. Equations (2) and (6) are functions of  $f_0$  which is also affected by bandwidth limitations and needs to be corrected (Mendecki and Niewiadomski, 1997). Corner frequency can be derived from the ratio  $P_v(n)/P_u(n)$  and therefore is  $f_0(n) = \sqrt{C(n)P_v(n)/P_u(n)}/(2\pi)$ , where  $C(n) = [(n-1)\sin(3\pi/n)]/[(n-3)\sin(\pi/n)]$ . Note that  $f_0(n)/f_0(n=2) = 1$ , which means that the corner frequency is the same for any  $n$ .

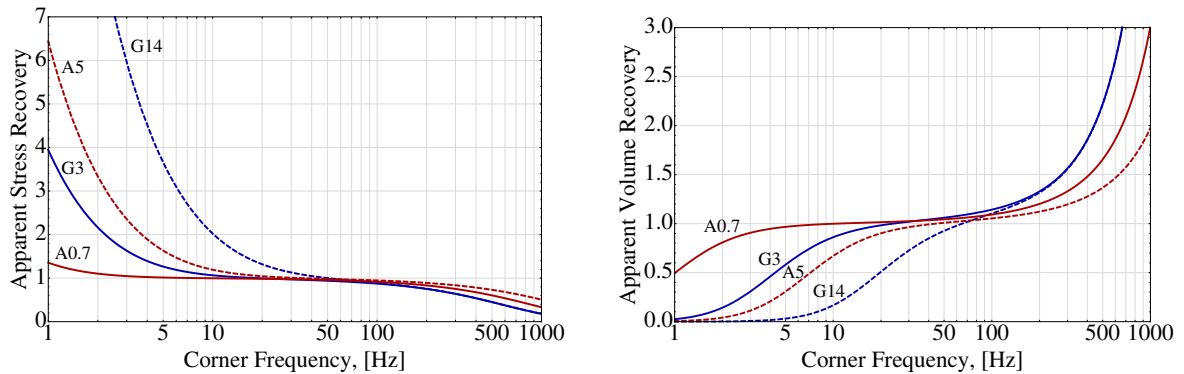


Figure 6: Over ( $> 1$ ) and under-estimates ( $< 1$ ) of  $\sigma_A$  (left) and  $V_A$  (right) as a function of  $f_0$  for the  $\omega^2$ -model for selected sensors defined by  $(f_1, f_2)$  [Hz]: 3 to 1000 (G3 – blue solid line), 14 to 1000 (G14 – blue dashed), 0.7 to 1500 (A0.7 – red solid) and 5 to 2300 (A5 – red dashed).

The  $\omega^2$ -model gives  $f_0(n=2) = \sqrt{P_v(n=2)/P_u(n=2)}/(2\pi)$ , see Andrews (1986). The recovery ratio for the  $\omega^2$ -model is

$$f_0(f_1, f_2) / f_0(f_1 = 0, f_2 = \infty) = \sqrt{1 + (B/A)}, \quad (7)$$

where  $f_0$  in  $A$  and  $B$  is calculated within the restricted frequency range  $(f_1, f_2)$ , see Figure 7. The best strategy though is to select the correct sensors for the range of potencies and energies to be recorded.

Seismic events occurring in mines are relatively small and the bulk of them are not recorded by the regional or national seismological networks that routinely estimate the local magnitude  $m_L$ . However, if there is a sufficient overlap between the mine and the national network one can calibrate parameters  $c_1$ ,  $c_2$  and  $c_3$  in  $m_L = c_1 \log E + c_2 \log P + c_3$ , to convert potencies and energies observed by the mine network to the  $m_L$  scale.

Here, poor recovery of seismic potency at low frequencies is partly compensated by better recovery of energy at higher frequencies. Such a calibration was done by *Butler* (1992), also reported by *Butler and van Aswegen* (1993) for the ISS system in South Africa and then re-evaluated by *Stankiewicz and Essrich* (2004). A quick survey of 100 mines in 12 countries revealed that 74 of them in 6 countries use the local magnitude defined by  $(c_1, c_2, c_3)$  for South African gold mines and the rest use the *Hanks and Kanamori* relation.

If the radiated seismic energy can be estimated reliably then  $\log E$  is the most appropriate measure of the strength of a seismic source and it should be used for seismic hazard assessment in mines. The second best option for hard rock mines is  $\log P$ . However, slow events in soft rock mines would result in larger potency magnitudes but be hardly perceptible because they would radiate little energy and produce low ground motion. Even in hard rock mines sources of seismic events associated with weaker geological features or with softer patches of rock yield more slowly under lower driving stresses and radiate over 100 times less seismic energy per unit of inelastic co-seismic deformation than equivalent sources associated with competent rock, see Figure 1.1 in *Mendecki* (1993).

$\log P$  can be converted to an energy magnitude assuming an average apparent stress for seismic events in mines, say 0.5 MPa, which gives  $m_E = \log E - 5.7$ . The energy magnitude,  $m_E$ , offers similar estimates to local magnitudes for larger seismic events in mines, but lower estimates for slower, less damaging events, see Table 2. For example event 870310 with local magnitude  $m_L$  1.4 radiated 16 times more energy than event 870131 with  $m_L$  1.5, and event 59 with  $m_{HK} - 2.3$  radiated 55 times more energy than event 94 with  $m_{HK} - 2.4$ . These differences are reflected in the energy based magnitudes.

All three,  $\log E$ ,  $\log P$  and  $m_E = \log E - 5.7$ , maintain the appropriate scaling for small earthquakes, are simple, independent of rigidity and easy to rescale to other potency or energy based relations, therefore one can objectively compare seismic hazard between different mines.

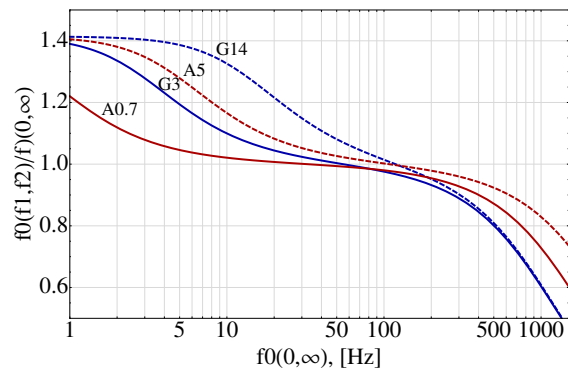


Figure 7: Over ( $> 1$ ) and under-estimates ( $< 1$ ) of  $f_0$  for the  $\omega^2$ -model due to sensor bandwidth limits  $(f_1, f_2)$  [Hz]: 3 to 1000 (G3 – blue solid line), 14 to 1000 (G14 – blue dashed), 0.7 to 1500 (A0.7 – red solid) and 5 to 2300 (A5 – red dashed).

Table 2: Source parameters and magnitude comparison for 10 well processed events. The first three are listed by *Gibowicz* (1982), 4 and 5 by *McGarr* (1994), 6, 7 and 8 by *Gibowicz et al.* (1990) and 9 and 10 by *Gibowicz et al.* (1991).

No.	Event	$\mu$ , GPa	$\log E$	$\log P$	$\sigma_A$ , MPa	$m_L$	$m_{HK}$	$m_e$	$m_E$
1	BLC	15.7	10.64	5.16	0.30	4.6	4.4	4.2	4.9
2	LBN	17.9	10.44	5.04	0.25	4.5	4.3	4.0	4.7
3	BTM-1	17.5	10.07	4.53	0.35	4.3	3.9	3.8	4.4
4	HBF-1	37.5	9.44	3.33	1.30	-	3.1	3.4	3.7
5	HBF-1a	37.5	8.85	2.86	1.00	-	2.8	3.0	3.1
6	870310	12.3	6.46	1.16	0.20	1.4	1.5	1.4	0.8
7	870112	12.3	6.37	1.29	0.12	1.5	1.7	1.4	0.7
8	870131	12.3	5.25	1.25	0.01	1.5	1.5	0.6	-0.4
9	59	30.6	1.50	-4.88	2.40	-	-2.3	-1.9	-4.2
10	94	30.6	-0.24	-5.08	0.69	-	-2.4	-3.1	-5.9



## Acknowledgements

I thank the anonymous reviewer for useful suggestions that made some statements more comprehensible. I thank Peter Mountfort for discussion on sensor characteristics and Ernest Lötter for data mining the magnitude relations at different mines and the average apparent stress. Dima Malovichko and Ernest Lötter internally reviewed the manuscript and Dima petitioned for a simple energy magnitude scale for mines.

## References

- Aki, K. (1969), Analysis of the seismic coda of the local earthquakes as scattered waves, *Journal of Geophysical Research*, 74(2), 615–631.
- Andrews, D. J. (1986), Objective determination of source parameters and similarity of earthquakes of different size, in *Earthquake source mechanics*, vol. 6, edited by S. Das, J. Boatwright, and C. H. Scholz, pp. 259–267, American Geophysical Monograph 37.
- Bakun, W. H., and A. G. Lindh (1977), Local magnitudes, seismic moments, and coda duration for earthquakes near Oroville, California, *Bulletin of the Seismological Society of America*, 67(3), 615–629.
- Ben-Menahem, A., and S. J. Singh (1981), *Seismic Waves and Sources*, Springer-Verlag, New York.
- Ben-Zion, Y., and L. Zhu (2002), Potency-magnitude scaling relation for southern California earthquakes with  $1.0 < M < 7.0$ , *Geophysical Journal International*, 148, F1–F5.
- Boatwright, J., and G. L. Choy (1986), Teleseismic estimates of the energy radiated by shallow earthquakes, *Journal of Geophysical Research*, 91, 2095–2112.
- Brune, J. N., R. J. Archuleta, and S. Hartzell (1979), Far-field S-wave spectra, corner frequencies, and pulse shapes, *Journal of Geophysical Research*, 84, May.
- Butler, A. G. (1992), Magnitude evaluation for mining regions using the Integrated Seismic System, *Internal Report 1992*, ISS International, Welkom, South Africa.
- Butler, A. G., and G. van Aswegen (1993), Ground velocity relationships based on a large sample of underground measurements in two South African mining regions, in *Proceedings 3rd International Symposium on Rockbursts and Seismicity in Mines, Kingston, Ontario, Canada*, edited by R. P. Young, pp. 41–50, Balkema, Rotterdam.
- Choy, G. L., and J. L. Boatwright (1995), Global patterns of radiated seismic energy and apparent stress, *Journal of Geophysical Research*, 100(B9), 18,205–18,228.
- Di Bona, M., and A. Rovelli (1988), Effects of the bandwidth limitation of stress drops estimated from integrals of the ground motion, *Bulletin of the Seismological Society of America*, 78(5), 1818–1825.
- Eshelby, J. D. (1957), The determination of the elastic field of an ellipsoidal inclusion and related problems, *Proceedings of the Royal Society of London, Series A, Mathematical and Physical Sciences*, 241(1226), 376–396.
- Gibowicz, S. J. (1963), Magnitude and energy of subterranean shocks in Upper Silesia, *Studia Geophys. Geod.*, 7, 1–19.
- Gibowicz, S. J. (1975), Variation of source properties: The Inangahua, New Zealand, aftershocks of 1968, *Bulletin of the Seismological Society of America*, 65(1), 261–276.

- Gibowicz, S. J. (1982), The mechanism of large mining tremors in Poland, in *Proceedings 1st International Symposium on Rockburst and Seismicity in Mines, Johannesburg, South Africa*, edited by N. C. Gay and E. H. Wainwright, pp. 17–28, South African Institute of Mining and Metallurgy.
- Gibowicz, S. J., H. P. Harjes, and M. Schafer (1990), Source parameters of seismic events at Heinrich Robert mine, Ruhr Basin, Federal Republic of Germany: Evidence for nondouble-couple events, *Bulletin of the Seismological Society of America*, 80(1), 88–109.
- Gibowicz, S. J., R. P. Young, S. Talebi, and D. J. Rawlence (1991), Source parameters of seismic events at the Underground Research Laboratory in Manitoba, Canada: Scaling relations for events with moment magnitude smaller than 2, *Bulletin of the Seismological Society of America*, 81(4), 1157–1182.
- Gutenberg, B., and C. F. Richter (1956a), Magnitude and energy of earthquakes, *Annals of Geophysics*, 9, 1–15.
- Gutenberg, B., and C. F. Richter (1956b), Earthquake magnitude, intensity, energy, and acceleration: (Second paper), *Bulletin of the Seismological Society of America*, 46(2), 105–145.
- Hanks, T. C., and H. Kanamori (1979), A moment magnitude scale, *Journal of Geophysical Research*, 84, 2348–2350.
- Kanamori, H., and D. L. Anderson (1975), Theoretical basis of some empirical relations in seismology, *Bulletin of the Seismological Society of America*, 65(5), 1073–1095.
- Keilis-Borok, V. I. (1959), On estimation of the displacement in an earthquake source and of source dimensions, *Annali di Geofisica*, 12(2), 205–214.
- Madariaga, R. (1979), On the relation between seismic moment and stress drop in the presence of stress and strength heterogeneity, *Journal of Geophysical Research*, 84(B5), 2243–2250.
- McGarr, A. (1994), Some comparisons between mining-induced and laboratory earthquakes, *Pure and Applied Geophysics*, 142(3-4), 467–489.
- Mendecki, A. J. (1993), Real time quantitative seismology in mines: Keynote Address, in *Proceedings 3rd International Symposium on Rockbursts and Seismicity in Mines, Kingston, Ontario, Canada*, edited by R. P. Young, pp. 287–295, Balkema, Rotterdam.
- Mendecki, A. J., and J. Niewiadomski (1997), Spectral analysis and seismic source parameters, in *Seismic Monitoring in Mines*, edited by A. J. Mendecki, 1 ed., chap. 8, pp. 144–158, Chapman and Hall, London.
- Mountfort, P., and A. J. Mendecki (1997), Seismic transducers, in *Seismic Monitoring in Mines*, edited by A. J. Mendecki, 1 ed., chap. 1, pp. 1–20, Chapman and Hall, London.
- Rautian, T. G. (1960), Earthquake energy, *Transaction of the Joint Institute of Physics of the Earth*, 9, 35–114.
- Stankiewicz, T., and F. Essrich (2004), Standardised local magnitude scale for South African mines, *Tech. rep.*, Anglo Gold Ashanti.
- Wierzchowska, Z., and J. Dubinski (1973), Methods to calculate energy of seismic events in Upper Silesia (in Polish), *Report*, Central Mining Institute, Katowice, Poland.
- Wyss, M., and J. N. Brune (1968), Seismic moment, stress and source dimensions for earthquakes in the California-Nevada region, *Journal of Geophysical Research*, 73(14), 4681–4694.